PSF Smooth Method based on Simple Lens Imaging

Dazhi Zhan, Weili Li, Zhihui Xiong, Mi Wang and Maojun Zhang
College of Information System and Management, National University of Defense Technology, Changsha, 410073, China
zhan938002@gmail.com

Keywords: Simple Lens Optics, Computational Photography, Chromatic Aberration, Point Spread Function, Image Deconvolution.

Abstract: Compared with modern camera lenses, the simple lens system could be more meaningful to use in many scientific applications in terms of cost and weight. However, the simple lens system suffers from optical aberrations which limits its applicapability. Recent research combined single lens optics with complex post-capture correction methods to correct these artifacts. In this study, we initially estimate the spatial variability point spread function (PSF) through blind image deconvolution with total variant (TV) regularization. PSF is optimized to be more smoothed for enhancing the robustness. A sharp image is then recovered through fast non-blind deconvolution. Experimental results show that our method is at par with state-of-the-art deconvolution approaches and possesses an advantage in suppressing ringing artifacts.

1 INTRODUCTION

Single lens optics with spherical surfaces often suffer from optical aberrations, such as geometric distortion, chromatic aberration, spherical aberration, and coma (Mahajan, 1991). These aberrations dramatically degrade image quality. Thus, modern cameras combine dozens of different lens elements to compensate aberrations. However, optical aberrations are inevitable, and the design of lenses always involves a trade-off among various parameters. A complicated lens combination has a significant effect on the cost and weight of camera objectives. With the recent development of unmanned aerial vehicles (UAVs) and motion cameras, such as the GoPro camera, simple lens systems appear to be achievable. The simple lens system still exhibits some unavoidable artifacts because of its structural defect. Recently, an alternative approach that utilizes single lens elements rather than a sophisticated lens design was developed through computational photography for high-quality imaging.

(Heide, 2013) and (Schuler, 2011) utilized a simple lens system with an image deconvolution method to achieve the image effect of single lens reflex (SLR) cameras. Their work provides a solution to the contradiction between image quality and complexity of imaging equipment. In the methods presented by Schuler and Heide, no pinhole light source, dark room, or complex image calibration and experimental process with high precision requirements is necessary to estimate PSF.

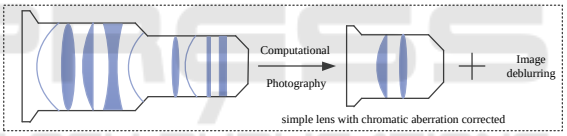

Figure 1: The correct mode based on simple lens optics.

In this work, we directly use a blind deconvolution method to estimate PSF. Given its spatial variability, the original image is divided into certain number of patches, and the PSF of each patch is estimated. According to the similarity of adjacent PSFs, each patch is processed with filters and rearranged to its previous arrangement to make the method robust and to suppress ringing artifacts. After estimating the spatially variable PSF, a fast non-blind deconvolution method is utilized to obtain a sharp image. Our work proves that acquiring high-quality images through a simple lens design and a computational photography method is possible. The simple lens system is potentially useful for many scientific applications, such as UAV imaging, astronomical imaging, remote sensing, and medical imaging.

The remainder of this paper is organized as follows. Section 2 provides a review of related work. Section 3 introduces direct PSF estimation by blind deconvolution, subsequent processing of the PSF filter, and a fast non-blind deconvolution method to restore sharp images. Section 4 presents the experi-

Zhan, D., Li, W., Xiong, Z., Wang, M. and Zhang, M.
PSF Smooth Method based on Simple Lens Imaging.
DOI: 10.5220/0006106100330038
In *Proceedings of the 6th International Conference on Pattern Recognition Applications and Methods (ICPRAM 2017)*, pages 33-38
ISBN: 978-989-758-222-6

ments and a comparison of the results of other methods. Section 5 provides the conclusion of the study.

2 RELATED WORK

2.1 Simple Lens Imaging

The idea of simple optics with computationally corrected aberrations was first proposed (Schuler, 2011). His work presented an approach to alleviate image degradations caused by imperfect optics; the approach can correct optical aberrations. In the calibration step, the optical aberrations are encoded in a spatially variant PSF in a completely dark room, with point light sources emitting light through a sufficiently small aperture. However, repeating the method is difficult because of the use of a highly complicated and sophisticated device to measure PSF. In addition, lens aberrations depend to a certain extent on the settings of the lens (aperture, focus, and zoom), which cannot be modeled trivially.

(Heide, 2013) referred to the research of Schuler and improved simple lens imaging. He proposed a new cross-channel prior for color images. This prior can handle large and complex blur kernel. Optimal first-order primal-dual convex optimization was used to incorporate the prior and guarantee global optimum convergence. With PSF estimation regarded as a deconvolution problem, Heide used a calibration pattern and a TV prior was used to ensure the robustness of per-channel spatially variant PSF estimation. However, their method requires highly sophisticated experimental procedures and a large amount of calculation time.

(Li, 2015) combined image and sparse kernel priors to estimate space-variant PSF in blind deconvolution and applied a fast non-blind deconvolution method based on the hyper-Laplacian prior to acquire a final clear image. Nevertheless, their method is unsuitable for solving chromatic aberrations.

2.2 Image Deconvolution

Although blind deconvolution is ill-posed, the problem still provides a fertile ground for novel processing methods. Blind image deconvolution approaches can be classified into two categories: separative and joint. In the separative approach, PSF is identified and later used to restore the original image in combination with a blurred image. This approach can generally be divided into two stages: blur kernel identification or PSF estimation and non-blind image deconvolution. The other class of existing deconvolution methods is the joint approach, in which the original image and blur kernel are identified simultaneously. Accordingly, several workaround methods, such as maximum a posterior (Stockham and Cannon, 1975), Bayesian methods (Lee and Cho, 2013), adaptive cost functions, alpha-matte extraction, and edge localization (Xu, 2013), are required to produce good results.

If PSF has been obtained, the problem is called non-blind deconvolution, in which image restoration is based on the problem of the blurred image and PSF. Compared with blind deconvolution, non-blind deconvolution solves a problem by employing a high-quality deconvolution algorithm. Evidently, directly using blurred images by dividing the kernel in the frequency domain does not work. Although PSF has been estimated, non-blind deconvolution remains an ill-posed problem. Ringing artifacts and loss of color would be observed even if a highly accurate kernel is provided.

Sparse natural image priors have been utilized to improve image restoration in non-blind deconvolution in which PSF is known (Cannon, 1976). Iteratively reweighted least squares (IRLS) (Levin and Fergus, 2007) and variable substitution schemes (Black and Rangarajan, 1996) have been employed to constrain the solution. To suppress ringing artifacts, Yuan et al. (Yuan and Sun, 2007) proposed a progressive procedure to gradually add back image details.

3 METHOD

In this chapter, we split the image into patches and estimate the spatially variant PSF through blind deconvolution. The blind deconvolution method proposed (Krishnan, 2011) is used to estimate the PSFs. The original l_1 regularization of k is a TV prior regularization to improve the accuracy of PSFs estimation. The processes of x and k update are introduced in Section 3.2. After the PSFs are estimated, they are smoothed by computing the weighted averages of neighboring patches(introduced in Section 3.3). Finally, a sharp image is obtained through fast non-blind deconvolution in Section 3.4.

3.1 Image Deblur Model

The primary challenge in achieving these goals is that simple lenses with spherical interfaces exhibit aberrations, i.e., high-order deviations from the ideal linear thin lens model. These aberrations cause rays from object points to focus imperfectly onto a single image point; Complicated PSFs that vary over the image plane are thus created. These PSFs need to be

removed through deconvolution. The effect becomes more pronounced at large apertures where many off-axis rays contribute to image formation. Many previous studies assumed that blurring is a spatially invariant convolution process.

$$B = I \otimes K \tag{1}$$

Where $\otimes$ is the convolution operator, I is the original image to recover, B is the observed blurred image and K is the blur kernel (or point spread function). The process of recovering the original image I from the blurred image B is the so-called image deblurring problem. The image degradation model is introduced, and its general regularization constraint model is:

$$\min_i ||i \otimes k - b||_2^2 + \lambda\phi(I) \tag{2}$$

The first term $||i \otimes k - b||_2^2$ is the fidelity term used to keep the matching degree between the clear image and the blurred image, so as to ensure the rationality of the image restoration result; the second term $\phi(I)$ is the regularization term. It contains prior knowledge on the kernel or original image; this prior information can guarantee that the characteristic of the restored image is similar to that of the clear image. λ is the regularization parameter, to balance the weight relation between the fidelity term and regularization.

3.2 Blind Kernel Estimation

In contrast to the simple lenses of Heide and Schuler, some improvements are achieved by adding one or two lenses, each of which is designed to correct the chromatic aberrations of a single lens. With the reduction in chromatic aberrations, the complexity of the PSF of the optical system also decreases. Different from PSF estimation with a calibration pattern (Heide, 2013; Brauers, 2010; Joshi, 2008),the current kernel estimation is performed in the images high-frequency region through blind deconvolution, in which a large amount of texture information of the image is obtained. Given the blurred and noisy patches of input image y, we generate the high-frequency version by using two discrete filters, namely, $\bigtriangledown x = [1,1]$ and $\bigtriangledown y = [1,1]^T$. The cost function for spatially-invariant blurring is:

$$\min_{x,k} ||x \otimes k - y||_2^2 + \frac{||x||_1}{||x||_2} + \mu||\bigtriangledown k||_1 \; s.t. \; k > 0, \sum_i k_i = 1 \tag{3}$$

The constraint on k that $k > 0, \sum_i k_i = 1$ enforces a non-negative and energy constraint. Here x is the unknown sharp image, k is the unknown blur kernel, and y is the input blurred noisy image. In the cost function, the first term $||x \otimes k - y||_2^2$ is a data-fitting term, The second term $\frac{||x||_1}{||x||_2}$ is the new regularization on x. The third term is a TV regularization of k. The form of PSF does not exhibit radial symmetry nor does it resemble a simple Gaussian shape or a disc shape. Thus, TV regularization is a robust approach for spatially variant PSF estimation. TV regularization helps to reduce the noise in the kernel which has good convergence properties, and μ is regularization parameters that balance the weight relation between the data-fitting term and kernel prior regularization.

The x sub-problem is expressed as follows:

$$\min_x ||x \otimes k - y||_2^2 + \frac{||x||_1}{||x||_2} \tag{4}$$

The new regularization term $\frac{||x||_1}{||x||_2}$ makes the sub-problem non-convex. Once the denominator from the previous iteration is fixed, the problem becomes a convex l_1 regularized problem. Numerous fast algorithms have been employed to solve l_1 regularized problems in compressed sensing literature, these algorithms include the well-known iterative shrinkage-thresholding algorithm (ISTA)(Beck and Teboulle, 2009). Krishnan reported that innerouter iteration is effective for convergence despite the non-convexity of a problem.

The k update sub-problem is expressed as follows:

$$\min_k ||x \otimes k - y||_2^2 + \mu||\bigtriangledown k||_1 \tag{5}$$

IRLS is used to solve the non-convexity problem. This method sets the invalid elements to zero and renormalizes the value to retain the constraints in the result of k. We perform IRLS once, and the kernel weight is computed from the kernel of the previous k update in the iterations. A low level of solving accuracy is obtained in the inner IRLS system by using several conjugate gradient (CG) iterations. During kernel optimization, after recovering the kernel at the finest level, we threshold small elements of the kernel to zero to reduce noise (Fergus, 2006).

3.3 Smoothed Spatially-variant PSF

Accurate estimation of PSF is essential to image deconvolution. An exact PSF can prevent the occurrence of the ringing effect in the image in the process of deconvolution. Previous studies usually assumed that PSF does not depend on the position in the image (spatially invariable PSF). However, because of the properties of optical systems, PSF changes as the position in the image varies (spatially variant PSF).

Fig.2(a) shows an internet protocol (IP) camera equipped with $1/1.9$" inches CMOS and images of

(a) (b)

Figure 2: (a) IP camera combined with C-mount (b) self-made simple lens with three lenses.

1080×1920 pixels can be obtained. Fig.2(b) show our self-made simple lens systems with three lenses at f/35mm. We capture the observed image with the simple lens system. Then, the images are split into 6×10 patches. Each patch of 180×192 pixels is estimated through blind convolution.

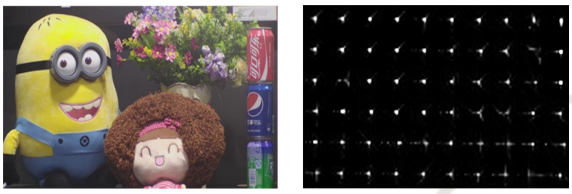

(a) (b)

Figure 3: (a) blurred image captured by three lenses (b) corresponding spatially-variant PSFs.

Fig.3 shows the image captured by our simple lens optics. On the right is PSF for various positions on the image plane, where each accumulation of points represents one PSF. As shown in the figure, PSF varies in different locations. Most of the kernels do not resemble a Gaussian shape, and the distribution does not exhibit radial symmetry. In addition, the kernels are highly spatially varying, ranging from disc-like structures to thin stripes (Brauers, 2010). Therefore, the shift-variant PSF can be modeled by

$$b(x,y) = i(x,y) \cdot k(x_0,y_0;x,y) + n(x,y) \qquad (6)$$

Where the sharp image is $i(x,y)$ and the blurred and noised image is $b(x,y)$. The spatially-varying PSF is expressed by $k(x_0,y_0;x,y)$,which related to the image patch location. Additional noise is modeled by $n(x,y)$.

Given that the image is divided into image patches, the number of pixels utilized to estimate PSF is reduced compared with the estimation that considers the entire image. Several incorrect PSF estimations are shown in Fig.3(b). The non-clustered region is spread, so the robustness and stability of the estimation are reduced.

We therefore propose a method to smooth the kernel through the neighboring PSFs. Considering that the optical system is gradually changing and the neighboring PSFs are similar, the weighted average of the blur kernel of different adjacent image patches is arranged consecutively in a new image. The pixels at the same position in each PSF are then rearranged into a new block. Each patch is processed with filters and rearranged to its previous arrangement. The filtering includes a 3×3 median filter, which reduces stochastic errors between neighboring patches. If the PSF estimation fails in one block or produces abnormal pixel values, the PSF data are obtained from neighboring PSFs.

The following low-pass filter of the filter kernel is defined by:

$$\begin{pmatrix} 1 & 2 & 1 \\ 2 & 4 & 2 \\ 1 & 2 & 1 \end{pmatrix} \qquad (7)$$

Next, several invalid values (the pixel values of PSF are below the dependent threshold) are set to zero. This procedure reduces the noise near the border of a PSF, in which only small values are expected. The function is defined by:

$$P(x,y) = \begin{cases} 0 & for \quad p(x,y) < T(x,y) \\ p(x,y) & for \quad p(x,y) \geq T(x,y) \end{cases} \qquad (8)$$

And the threshold function:

$$T(x,y) = 1 - H(x)H(y) \qquad (9)$$

$$H(d) = \begin{cases} 1 & for \quad 0 \leq d \leq \alpha\frac{R}{2} \\ 1 - [\frac{d-\alpha\frac{R}{2}}{2(1-\alpha)\frac{R}{2}}]^2 & for \quad \alpha\frac{R}{2} < d \leq \frac{R}{2} \end{cases} \qquad (10)$$

Where $P(x,y)$is the smooth PSF value of current pixel, the d is the distance between the pixel and the center of the blur kernel, and the R is the size of kernel. Parameter $\alpha(0 < \alpha < 1)$ control the intensity of the noise reduction.

3.4 Fast Non-blind Deconvolution

Once the final kernel k is estimated, the problem changes to non-blind deconvolution that recovers the sharp image x from y. Krishnan opted to use the non-blind deconvolution method from [12]. This algorithm uses a continuation method to solve the following cost function:

$$\min_{x,k} ||x \otimes k - y||_2^2 + \mu|| \bigtriangledown_g y||_{0.8} \qquad (11)$$

Where $\bigtriangledown_g$ is the horizontal and vertical derivative filters:$\bigtriangledown_x = [1,-1]$ and $\bigtriangledown_y = [1,-1]^T$. It can also be

useful to include second order derivatives, or the more sophisticated filters (Roth and Black, 2005). The $l_{0.8}$ norm is set to distribute derivatives equally over the image, and a sparse prior is selected to concentrate derivatives at a small number of pixels, thus leaving the majority of image pixels constant (Levin and Fergus, 2007). This condition produces sharp edges, reduces noise, and helps remove unwanted image artifacts, such as ringing.

The state-of-the-art single image deblurring method proposed by Xu et al(Xu, 2013). They propose a generalized and mathematically sound l_0 sparse expression. In next chapter our test results are then compared with Xu's to demonstrate the process and determine improvements for our method

4 RESULTS

This section presents detailed comparisons of deconvolution methods to correct current single lens aberration. The actual tested images are all obtained at ISO 100 and auto exposure. We implement our algorithm and conduct experiments in MATLAB. All experiments are performed on a computer with dual-core Intel Core i5 CPU with 2.7 GHz and 8 GB RAM.

Test images with a size of 1080×1920 were captured with an IP camera using our simple lens system with three individual elements. The PSF estimated with Xus method is space-invariant, and its size is approximated by an algorithm. Meanwhile, the PSF size in our method is fixed to 21. The parameters in Xu's method are set to the combination that produces the best deconvolution result. The computing time of our method is 338 seconds and Xu's method is 29 seconds.

The image captured by the simple lens system is shown in Fig.4, the Fig.4(a) is original image exhibiting texture loss because of chromatic aberration. After the deconvolution process, Xu's method can restore most of the contours of the image and can correct chromatic aberration. However, as observed in the left close-up window in Fig.4(b), Xu's method allows ringing artifacts, particularly in the high-frequency region. For example, around the red character in the yellow background, undue transverse corrugations between two characters are generated. By comparison, our method (Fig.4(c)) is clean and preserves more details. Ringing artifacts usually occur because of the inaccurate estimation of PSF. By estimating the spatially varying PSF and smoothing, our method ensures robustness and restores the blurred image while suppressing ringing artifacts during deconvolution.

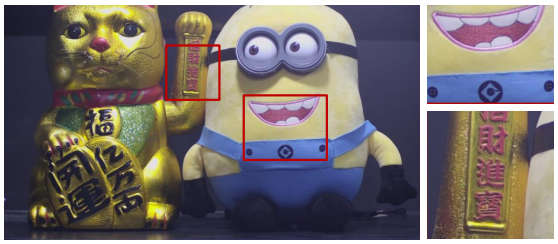

(a)Input image

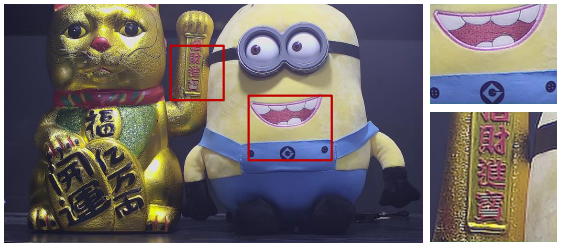

(b)Xu's method

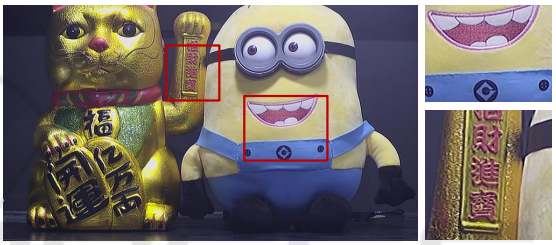

(c)Our method

Figure 4: Deconvolution result comparison of real images. (a) Input blurred images captured by simple lens camera with three lenses. (b) The deblurred result(Xu, 2013). (c) The deblurred result by our approach.

To increase the credibility of the results, we compare another set of images under a different light condition. The same conclusions are obtained. Comparison of the characters on the bottle and eyes of the yellow minion shows that slight out-of-focus blur and ringing artifacts still exist (Fig.5(b)). With regard to the hair and flower region, our method restores small edges and preserves texture details because of the accurate estimation of PSF. Our method outperforms previous single image deblurring methods in terms of total visual quality and details.

5 CONCLUSION

By adding one or two individual optics to optimize the lens design and implementing sufficient blind deconvolution, we proved that single lens imaging, which suffers from optical aberrations, can eliminate chromatic aberrations and restore a sharp image.

We estimated spatially variant PSFs through blind deconvolution with a TV prior and smoothed the PSFs

(a)Input image

(b)Xu’ s method

(c)Our method

Figure 5: Deconvolution result comparison of another set of images. (a) Input blurred images captured by simple lens camera with three lenses. (b) The deblurred result (Xu, 2013). (c) The deblurred result by our approach.

by using neighboring image patches. This method of PSF estimation is robust and highly efficient. Then, we restored a sharp image through non-blind deconvolution, and the results are comparable with those of state-of-the-art deconvolution approaches. Our method has an advantage in suppressing ringing artifacts and recovering edge details.

Further improvement can be explored by establishing a more reasonable means of image division, such as dividing the image according to the texture or frequency domain. Another aspect is the current 2D-PSF estimation; future work can estimate 3D-PSF with image depth of field.

REFERENCES

Beck, A. and Teboulle, M. (2009). Fast iterative shrinkage-thresholding algorithm for linear inverse problems. In *Siam Journal on Imaging Sciences, 2 (1), 233-240.*

Black, M. and Rangarajan, A. (1996). The unification of line processes, outlier rejection and robust statistics with applications to early vision. In *International Journal of Computer Vision.*

Brauers, J. (2010). Direct psf estimation using a random noise target. In *SPIE Electronic Imaging, July.*

Cannon, M. (1976). Blind deconvolution of spatially invariant image blurs with phase. In *IEEE Trans. Acoust. Speech, Signal Processing, vol. 24, p. 5863.*

Fergus, R. (2006). Camera shake from a single photograph. In *Acm Transactions on Graphics, 25 (3), 787-794.*

Heide, F.and Rouf, M. (2013). High-quality computational imaging through simple lenses. In *Acm Transactions on Graphics, 32 (5), 13-15.*

Joshi, N. (2008). Psf estimation using sharp edge prediction. In *IEEE Conference on Computer Vision and Pattern Recognition, CVPR, 18 23-28.*

Krishnan, D. (2011). Blind deconvolution using a normalized sparsity measure. In *IEEE Conference on Computer Vision Pattern Recognition, 233-240.*

Lee, S. and Cho, S. (2013). Recent advances in image deblurring. In *SIGGRAPH Asia, 1-108.*

Levin, A. and Fergus, R. (2007). Deconvolution using natural image priors. In *26 (3).*

Li, W.and Liu, Y. (2015). Computational photography algorithm for quality enhancement of single lens imaging deblurring. In *Optik-International Journal for Light and Electron Optics, 126 (21), 2788-2792.*

Mahajan, V. (1991). *Aberration Theory Made Simple.* Canada.

Roth, S. and Black, M. (2005). A frame- work for learning image priors. In *In CVPR.*

Schuler, C.J.and Hirsch, M. (2011). Non-stationary correction of optical aberrations. In *International Conference on Computer Vision, 32, 659-666.*

Stockham, T. and Cannon, T. (1975). Blind deconvolution through digital signal processing. In *Proceedings of the IEEE, 63 (4), 678-692.*

Xu, L. (2013). Unnatural l0 sparse representation for natural image deblurring. In *IEEE Conference on Computer Vision Pattern Recognition, 1107-1114.*

Yuan, L. and Sun, J. (2007). Image deblurring with blurred/noisy image pairs. In *ACM SIGGRAPH. vol.26, pp.1.*